Research article

JHEP|Reports

ROCK2 inhibition attenuates profibrogenic immune cell function to reverse thioacetamide-induced liver fibrosis

Christina Nalkurthi,[1,2] Wayne A. Schroder,[1] Michelle Melino,[1] Katharine M. Irvine,[3] Melanie Nyuydzefe,[4] Wei Chen,[4] Jing Liu,[1] Michele W.L. Teng,[1] Geoffrey R. Hill,[5] Patrick Bertolino,[6] Bruce R. Blazar,[7] Gregory C. Miller,[8] Andrew D. Clouston,[8] Alexandra Zanin-Zhorov,[9,†] Kelli P.A. MacDonald[1,*,†]

[1]*QIMR Berghofer Medical Research Institute, Brisbane, Australia;* [2]*The University of Queensland, Brisbane, QLD, Australia;* [3]*Mater Research, Translational Research Institute, University of Queensland, Brisbane, Australia;* [4]*Kadmon Corporation LLC, New York, NY, USA;* [5]*Clinical Research Division, Fred Hutchinson Cancer Research Centre, Seattle, WA, USA;* [6]*Centenary Institute, Sydney, Australia;* [7]*Masonic Cancer Center and Division of Blood and Marrow Transplantation, Department of Pediatrics, University of Minnesota, Minneapolis, MN, USA;* [8]*Envoi Specialist Pathologists, Brisbane, Australia;* [9]*Equilibre BioPharmaceuticals LLC, New York, NY, USA*

JHEP Reports **2022.** https://doi.org/10.1016/j.jhepr.2021.100386

Background & Aims: Fibrosis, the primary cause of morbidity in chronic liver disease, is induced by pro-inflammatory cytokines, immune cell infiltrates, and tissue resident cells that drive excessive myofibroblast activation, collagen production, and tissue scarring. Rho-associated kinase 2 (ROCK2) regulates key pro-fibrotic pathways involved in both inflammatory reactions and altered extracellular matrix remodelling, implicating this pathway as a potential therapeutic target.
Methods: We used the thioacetamide-induced liver fibrosis model to examine the efficacy of administration of the selective ROCK2 inhibitor KD025 to prevent or treat liver fibrosis and its impact on immune composition and function.
Results: Prophylactic and therapeutic administration of KD025 effectively attenuated thioacetamide-induced liver fibrosis and promoted fibrotic regression. KD025 treatment inhibited liver macrophage tumour necrosis factor production and disrupted the macrophage niche within fibrotic septae. ROCK2 targeting *in vitro* directly regulated macrophage function through disruption of signal transducer and activator of transcription 3 (STAT3)/cofilin signalling pathways leading to the inhibition of pro-inflammatory cytokine production and macrophage migration. *In vivo*, KDO25 administration significantly reduced STAT3 phosphorylation and cofilin levels in the liver. Additionally, livers exhibited robust downregulation of immune cell infiltrates and diminished levels of retinoic acid receptor-related orphan receptor gamma (RORγt) and B-cell lymphoma 6 (Bcl6) transcription factors that correlated with a significant reduction in liver IL-17, splenic germinal centre numbers and serum IgG.
Conclusions: As IL-17 and IgG–Fc binding promote pathogenic macrophage differentiation, together our data demonstrate that ROCK2 inhibition prevents and reverses liver fibrosis through direct and indirect effects on macrophage function and highlight the therapeutic potential of ROCK2 inhibition in liver fibrosis.
Lay summary: By using a clinic-ready small-molecule inhibitor, we demonstrate that selective ROCK2 inhibition prevents and reverses hepatic fibrosis through its pleiotropic effects on pro-inflammatory immune cell function. We show that ROCK2 mediates increased IL-17 production, antibody production, and macrophage dysregulation, which together drive fibrogenesis in a model of chemical-induced liver fibrosis. Therefore, in this study, we not only highlight the therapeutic potential of ROCK2 targeting in chronic liver disease but also provide previously undocumented insights into our understanding of cellular and molecular pathways driving the liver fibrosis pathology.

Introduction

Chronic liver disease (CLD) is a progressive destruction of the liver and is a significant global health burden. CLD occurs in response to injury induced by multiple insults such as alcohol exposure, obesity, diabetes, viral infection, autoimmunity, chronic inflammatory conditions, and drug toxicity. Fibrosis is the hallmark of CLD, and its progression eventually results in cirrhosis and diminished organ function and can lead to hepatocellular carcinoma (HCC). Although recent evidence suggests that fibrosis is a reversible process, there are currently limited antifibrotic treatments available.

Rho-associated coiled-coil forming protein kinases (ROCK) are established mediators of fibrosis in multiple disease settings. Two mammalian isoforms exist, ROCK1 and ROCK2, both of which are activated by the small GTPase Rho[1] in response to several pro-fibrotic stimuli such as transforming growth factor-beta (TGF-β), lysophosphatidic acid, and extracellular matrix

Keywords: Liver fibrosis; ROCK2; Inflammation; Macrophages; IL-17; B cells; Therapy.
Received 21 February 2021; received in revised form 27 September 2021; accepted 29 September 2021; available online 6 October 2021
† These authors are equal contributors.
* Corresponding author. Address: QIMR Berghofer Medical Research Institute, 300 Herston Rd, Brisbane, 4006. Australia. Tel.: +61-7-3362-0404.
E-mail address: Kelli.MacDonald@qimrberghofer.edu.au (K.P.A. MacDonald).

(ECM) stiffness.[2,3] ROCK-mediated effects are elicited by phosphorylation of downstream targets including myosin light chain, LIM kinase, and cofilin, which are all associated with the regulation of actin cytoskeleton dynamics and cell contractility.[4] These processes underpin multiple cellular functions including cell migration activation, differentiation, and survival. ROCK1/2 inhibition has been demonstrated to ameliorate fibrosis in experimental models of pulmonary,[5] cardiac,[6] renal,[7] and liver fibrosis.[8] Thus, ROCK activity plays a key role in the development of fibrosis in most organs. Although ROCK1 and ROCK2 exhibit a high degree of homology,[9] they are functionally non-redundant. Recently, it was reported that selective ROCK2 inhibition efficiently prevented development of lung[10] and renal[11] fibrosis in animal models. Thus, ROCK2 targeting offers the therapeutic approach to reduce organ fibrosis without the profound effects of dual ROCK1/2 inhibition and potential harmful outcomes in patients. Although both isoforms have been implicated in fibrogenesis, the efficacy of isoform-specific targeting and the distinct mechanisms by which the specific ROCK isoforms contribute to the pathophysiology of hepatic fibrosis remain an enigma.

Chronic inflammation in CLD is known to drive the development of fibrosis in this condition. Although both ROCK1 and ROCK2 are expressed in immune cells, only ROCK2 regulates the secretion of the pro-inflammatory cytokine interleukin IL-17A (hereafter referred to as IL-17) through the phosphorylation of signal transducer and activator of transcription 3 (STAT3) and expression of downstream transcription factors such as retinoic acid receptor (RAR)-related orphan receptor gamma (RORγt).[12] IL-17 contributes to liver fibrogenesis through multiple mechanisms, including through the direct activation of hepatic stellate cells (HSCs) to promote the synthesis of collagen.[13] ROCK2 signalling also promotes B-cell lymphoma 6 (BCL6) expression and IL-21 secretion in T follicular helper (Tfh) cells that, in turn, provide survival signals to germinal centre (GC) B cells to promote pathogenic Ig production.[14]

Multiple lines of evidence indicate that macrophages, both liver-resident Kupffer cells and infiltrating monocyte-derived macrophages, mediate inflammation and drive liver fibrosis. During chronic injury, these liver-associated macrophages trigger HSC activation and differentiation into collagen-producing myofibroblasts by releasing pro-fibrotic mediators such TGF-β, tumour necrosis factor (TNF), and platelet-derived growth factor.[15] IL-17A directly promotes the pathogenic differentiation and function of macrophages, including Kupffer cells, via STAT3-dependent mechanisms.[16] Moreover, IL-17 also acts as a chemokine to recruit monocytes and macrophages.[17,18] Importantly, ROCK2 signalling has been recently shown to drive macrophage differentiation and induce pro-inflammatory responses in a cell-intrinsic manner both *in vitro* and *in vivo*.[19,20] Thus, the ROCK2 pathway appears to have a broad role in pro-inflammatory signal transduction to promote the pathogenic function of T cells, B cells, and macrophages in the context of fibrosis.

Here, we have investigated the antifibrotic potential of KD025, a potent, orally available selective ROCK2 inhibitor, in the thioacetamide (TAA)-induced liver fibrosis mouse model, which closely resembles injury observed in patients with hepatitis with only mild elevation in alanine aminotransferase (ALT)/aspartate aminotransferase (AST) despite fibrosis development.[21] Oral administration of TAA induces a gradual progressive liver disease characterised by inflammation, ductular reaction (DR), extensive fibrosis, and eventual progression to HCC, thus mimicking the inflammation/fibrosis/malignancy disease progression that occurs in patients.[22] Our data demonstrate the striking efficacy of targeted ROCK2 inhibition in both prevention and reversal of liver fibrosis in the TAA model through direct and indirect effects on macrophage profibrogenic function.

Materials and methods

Mice

Female C57BL/6 (B6.wild-type [WT]) mice were purchased from the Animal Resources Centre (Perth, Western Australia, Australia). B6. $\mu mt^{-/-}$[23] B6. $Fc\gamma R^{-/-}$, and B6. IL-$17A^{-/-}$[24] mice were bred and housed at QIMR Berghofer Medical Research Institute (Brisbane, Australia). IL-17^{Cre} and $Rosa26^{eYFP}$ mice were provided by Brigitta Stockinger (Francis Crick Institute, London UK) and crossed to generate IL-$17^{cre}Rosa26^{eYFP}$ heterozygous mice.[25] Mice were housed in sterilised micro-isolator cages and received acidified autoclaved water (pH 2.5) and normal chow. Mice were treated with or without TAA (Sigma-Aldrich, St. Louis, MO, USA) supplemented in the drinking water at 300 mg/L for 1–8 weeks. Where indicated, mice were given KD025 (100 mg/kg per animal daily by oral gavage, selected based on the most effective dose in our earlier chronic graft-*vs*-host disease (cGVHD) animal studies[14]) or 0.4% methylcellulose vehicle from Days 0–6 or Days 42–54. KD025 was kindly provided by Kadmon Pharmaceuticals. All animal experiments were approved by and performed in accordance with the QIMR Berghofer Animal Ethics Committee.

Histology

At time points indicated, livers were harvested, formalin-preserved, embedded in paraffin, and processed to generate 5-μm-thick sections. H&E and Sirius red (SR) stained sections were examined in a blinded fashion (by ADC and GCM) to assess the inflammatory infiltrate and degree of fibrosis. Collagen proportional area on SR-stained slides was measured using Aperio analysis algorithm in ImageScope software version 11.2 (Aperio, Sausalito, USA). A total of 3 separate areas (5–10 mm^2) were analysed for each sample, excluding the capsule and portal tracts larger than 150 mm.

Isolation of hepatic leucocytes

For the isolation of hepatic leucocytes, livers were perfused with 1 mg/ml collagenase IV (Sigma) and 0.1 mg/ml DNase I (Sigma) in HBSS (Sigma) and minced finely and fragments incubated at 37°C for 40 min in collagenase IV/DNase I solution. After incubation, the cell suspension was pressed through a 70-μM cell strainer (Becton Dickinson, New Jersey, USA), washed twice in cold FACS buffer (PBS containing 2% heat-inactivated FBS and 0.5 mM EDTA), resuspended in 33% Percoll gradient (Percoll, BIO-STRATEGY PTY LIMITED, Brisbane, Australia) in PBS, and centrifuged at 600*g* for 15 min with no brake. The supernatant containing hepatocytes was discarded, and the resulting non-parenchymal cell pellet was subjected to red cell lysis using Gey's solution, washed twice, and resuspended in cold FACS buffer.

Cell staining and flow cytometry

Isolated hepatic leucocytes (10^6) were incubated with 2.4G2 (BD Biosciences, San Diego, CA, USA) for 10 min to block Fc

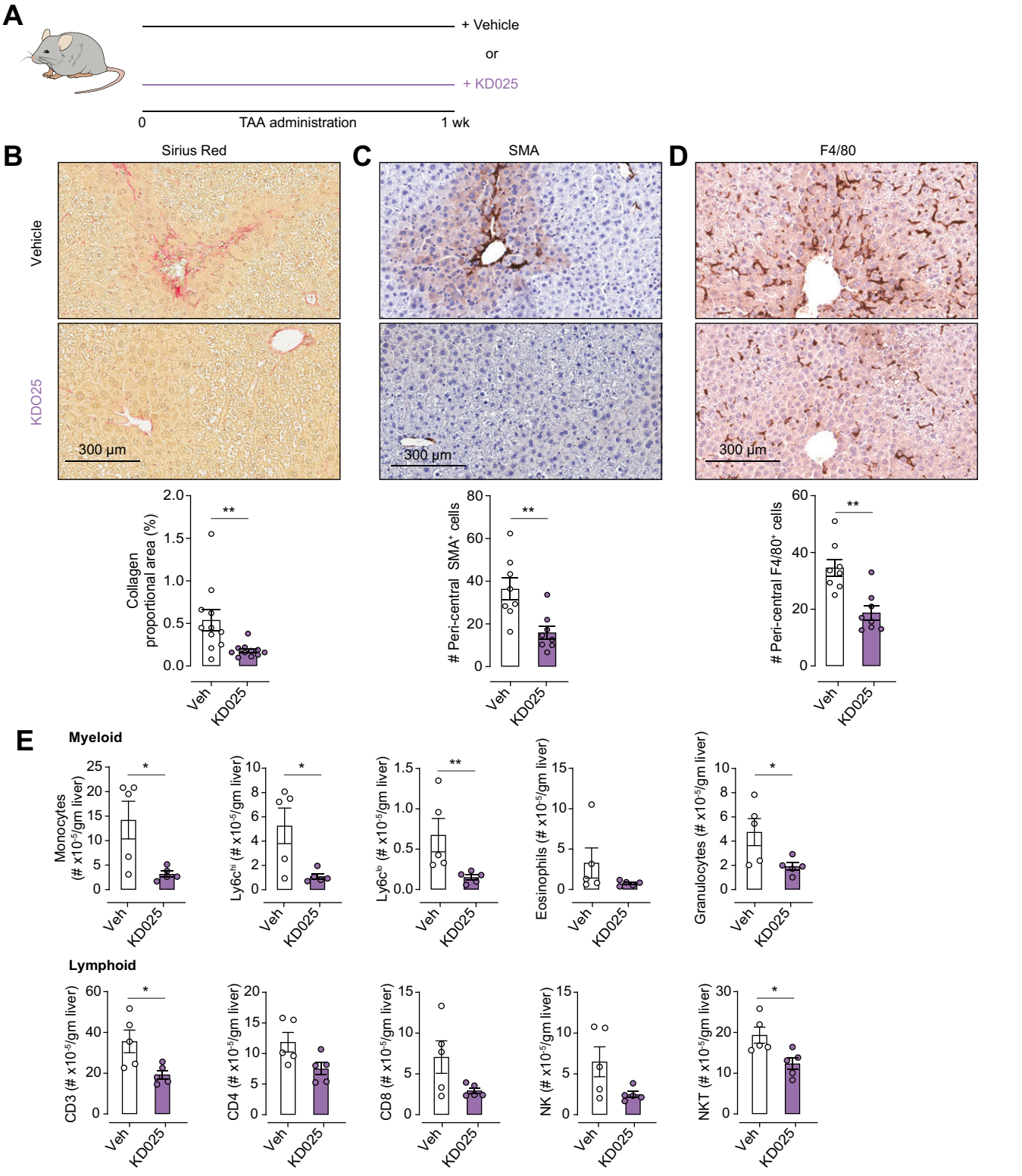

Fig. 1. KDO25 inhibits TAA-induced liver fibrosis. (A) C57BL/6 mice were treated for 1 week with TAA and vehicle or TAA and KD025 co-administration. Histochemical staining and Aperio quantification of liver sections were undertaken for (B) SR, (C) SMA, and (D) F4/80 (n = 8–11 animals/group; combined from 2 independent experiments). Representative images are shown. (E) Absolute number of liver myeloid and lymphoid cells in mice treated as in (A) was determined by flow cytometry (n = 5 animals/group). Data are presented as mean ± SEM. $^{*}p$ <0.05, $^{**}p$ <0.01 Mann–Whitney *U* test. SMA, smooth muscle actin; SR, Sirius red; TAA, thioacetamide.

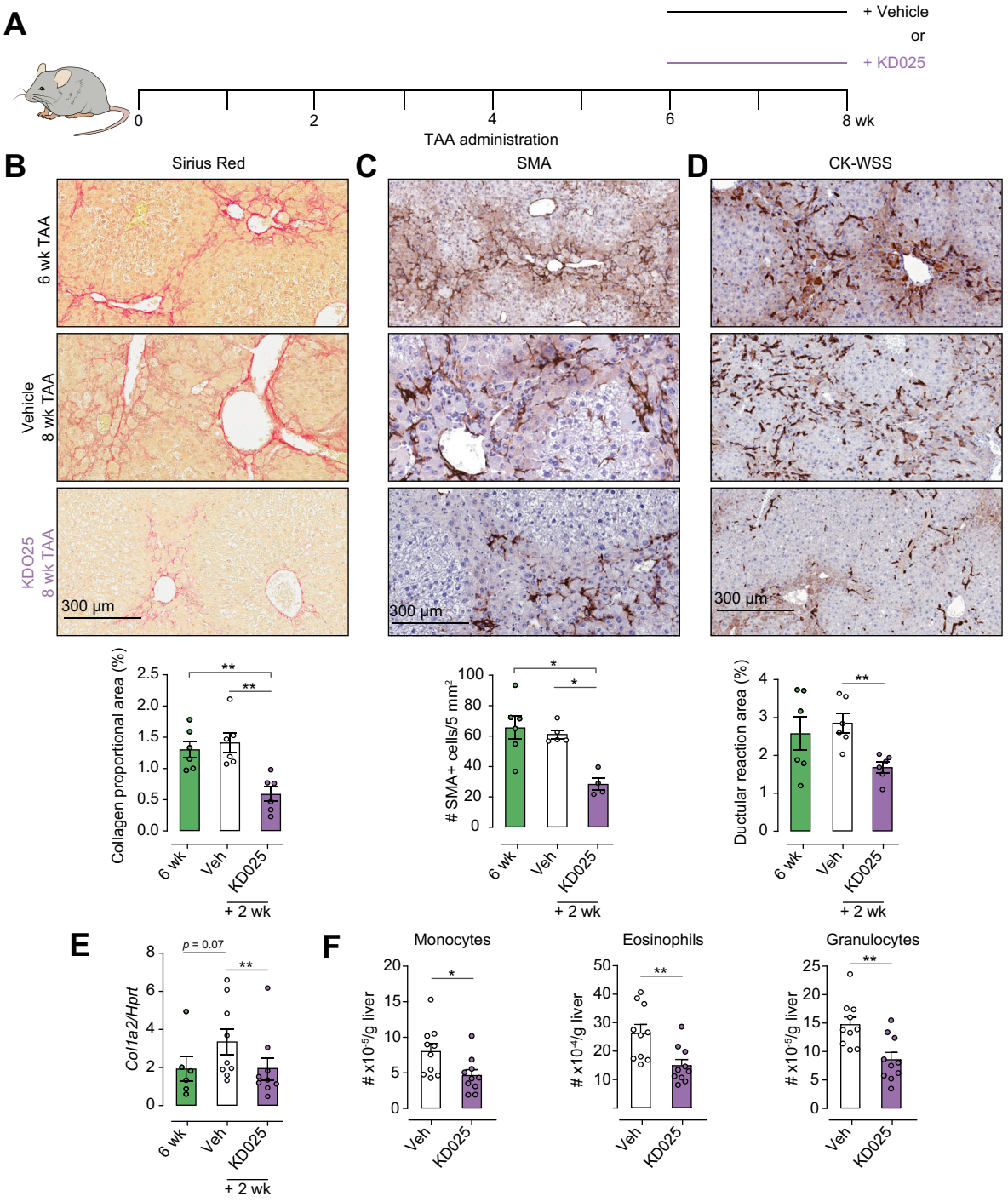

Fig. 2. KDO25 promotes regression of TAA-induced liver fibrosis. (A) C57BL/6 mice were treated with TAA for 6 weeks followed by 2 weeks of TAA and vehicle or TAA and KD025 co-administration. Histochemical staining and Aperio quantification of (B) SR, (C) SMA, and (D) pan-keratin (CK-WSS) in liver sections were undertaken (n = 4–6 animals/group). Representative images are shown. (E) Expression of *col-1a* mRNA in whole liver was determined by qRT-PCR and normalised to *HPRT* mRNA levels (n = 6–9 animals/group; combined from 2 independent experiments). (F) Absolute number of monocytes, eosinophils, and granulocytes was determined by flow cytometry (n = 10 animals/group; combined from 2 independent experiments). Representative images, and data are presented as mean ± SEM. *p <0.05, **p <0.01 Mann–Whitney U test. qRT-PCR, quantitative real-time PCR; SMA, smooth muscle actin; SR, Sirius red; TAA, thioacetamide; WSS, wide spectrum screening.

receptor binding before staining with lineage specific antibodies for phenotyping. Intracellular cytokine (ICC) staining was performed by stimulating hepatic leucocytes (5×10^6) for 4 h at 37°C with PMA (5 µg/ml) and ionomycin (50 µg/ml) (Sigma-Aldrich) along with Brefeldin A (BioLegend, San Diego, USA) before surface staining, followed by cell fixation, permeabilisation (BD Cytofix/Cytoperm kit), and cytokine staining. All samples were acquired on a BD LSR Fortessa (BD

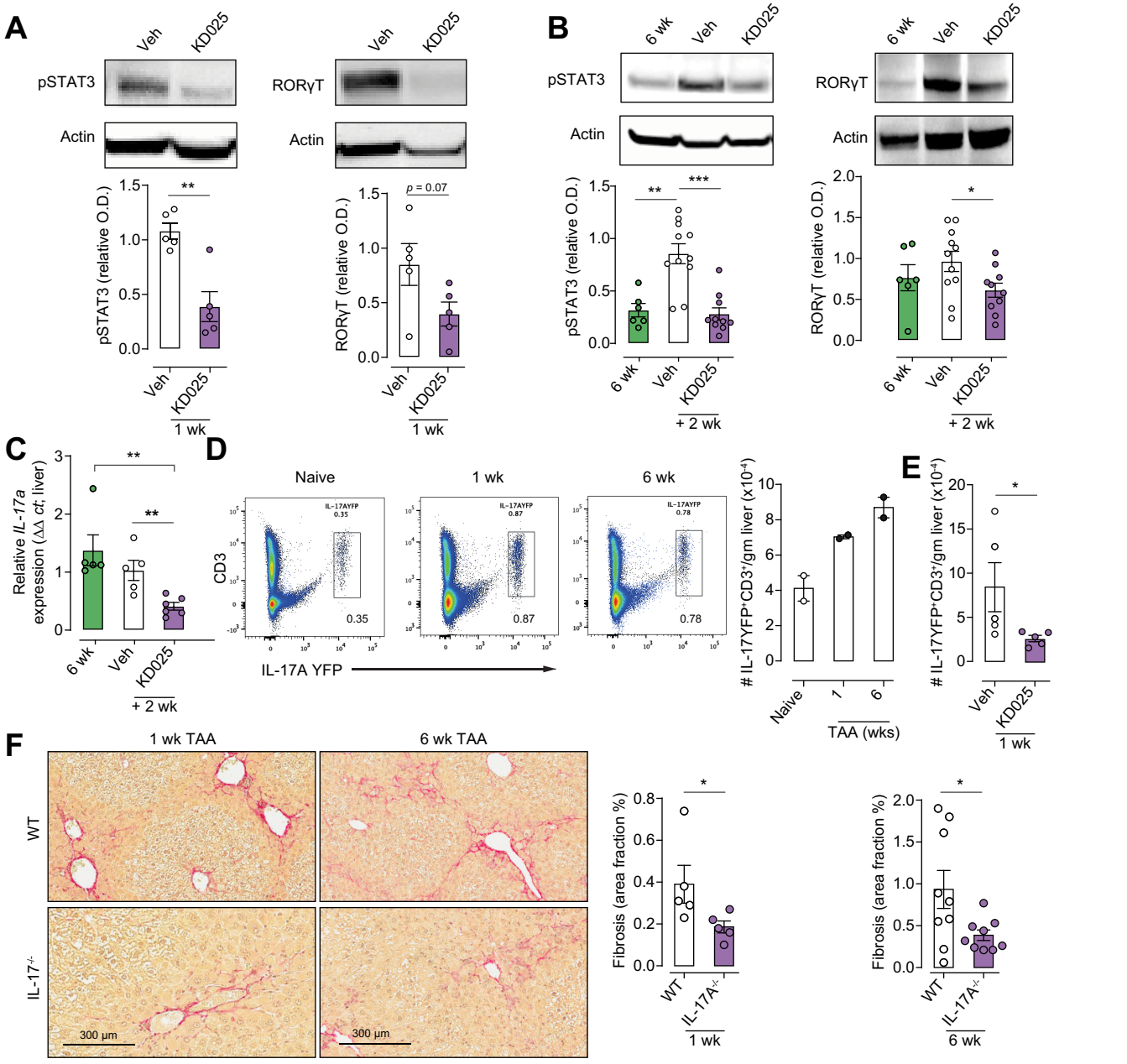

Fig. 3. KDO25 inhibits pSTAT3, RORγt, and IL-17A expression in liver. (A) Liver lysates of C57BL/6 mice, treated for 1 week with TAA and vehicle or with TAA and KD025, were analysed by immunoblot using antibodies specific for phosphorylated STAT3^{Y705} (pSTAT3), RORγt, and actin. Densitometric analysis of pSTAT3 and RORγt normalised to actin is shown (n = 5 animals/group). (B) Mice treated with TAA for 6 weeks or treated with TAA for 6 weeks followed by 2 weeks of coadministration with 0.4% methylcellulose (veh) or 100 mg/kg KDO25, were analysed as in (A) (n = 6–11 animals/group). (C) IL-17a mRNA expression in mice treated as in (B) was determined by qRT-PCR and normalised to HPRT mRNA levels (n = 5–6 animals/group). (D) Livers of IL-17A^{YFP} fate reporter mice left untreated (naïve) or treated with TAA for 1 or 6 weeks were analysed for IL-17A-YFP and CD3 expression by flow cytometry. Representative dot plots and the number of IL-17-YFP+/CD3+ cells are shown (n = 2 animals/group). (E) IL-17A-YFP fate reporter mice treated for 1 week with TAA and 0.4% methylcellulose (veh) or with TAA and 100 mg/kg KDO25 were analysed as in (D) (n = 5 animals/group). (F) WT and IL-17A$^{-/-}$ mice treated with TAA for 1 or 6 weeks, and liver sections were analysed by histochemical staining and Aperio quantification of Sirius red. Representative liver sections and quantitation of collagen are shown (n = 5–9 animals/group; combined from 2 independent experiments). Data are presented as mean ± SEM. *p <0.05, **p <0.01, ***p <0.001 Mann–Whitney U test. O.D., optical density; pSTAT3, signal transducer and activator of transcription 3 phosphorylation; qRT-PCR, quantitative real-time PCR; RORγt, retinoic acid receptor-related orphan receptor gamma; SMA, smooth muscle actin; SR, Sirius red; TAA, thioacetamide; WT, wild type.

Biosciences) and analysed using FlowJo software (v10, FlowJo, LLC. Ashland, USA). The absolute number of each cell type was calculated by multiplying the frequency by the total number of hepatic leucocytes per gram liver.

IncuCyte scratch wound cell migration assay

Bone marrow-derived macrophages (BMDM; 10^6) were seeded onto wells of 96-well plates (ImageLock, Essen Bioscience Inc., Ann Arbor, MI, USA) and cultured in 30% L cell conditioned

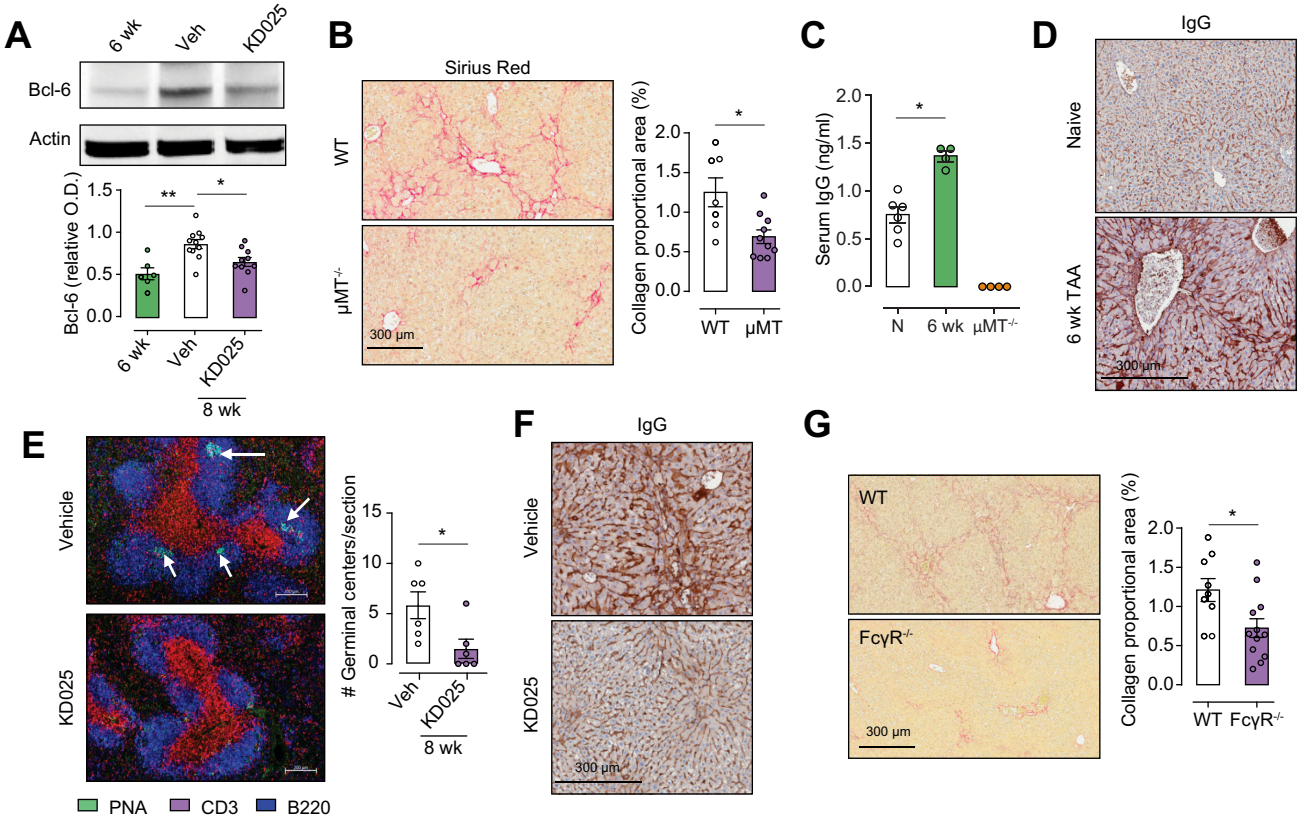

Fig. 4. KDO25 inhibits Bcl6 expression, germinal centre formation, and Ig deposition in B cells. (A) Mice treated with TAA for 6 weeks or treated with TAA for 6 weeks followed by 2 weeks of co-administration with vehicle or KD025 were analysed by immunoblot for Bcl6 and actin expression. Densitometric analysis of Bcl6 levels normalised to actin is shown (n = 6–11 animals/group). (B). C57BL/6 WT and μMT$^{-/-}$ mice were treated with TAA for 6 weeks, and liver sections were analysed by histochemical staining and Aperio quantification of SR. Representative liver sections and quantitation of collagen are shown (n = 7–10 animals/group; combined from 2 separate experiments). (C) C57BL/6 WT and μMT mice were treated with TAA for 6 weeks. These and untreated WT mice (N) were analysed by ELISA for serum Ig levels (n = 4–6 animals/group). (D) C57BL/6 mice were left untreated (naïve) or were treated with TAA for 6 weeks, and liver sections were analysed by histochemical staining for Igs. (E) Mice were treated with TAA for 6 weeks or treated with TAA for 6 weeks followed by 2 weeks of co-administration with vehicle or KD025. Spleens were analysed for germinal centre formation by immunofluorescent staining with anti-CD3 (red), anti-B220 (blue), and carbohydrate PNA (green) followed by confocal microscopy (n = 6 animals/group). (F) Histochemical staining for immunoglobulin deposition (IgG) in the liver of mice treated for 6 weeks with TAA co-administered with vehicle or KD025. (G) WT and FcγR$^{-/-}$ mice were treated with TAA for 6 weeks followed by histochemical staining and Aperio quantification of SR. Representative liver sections are shown with SR quantification presented as mean ± SEM (n = 9–12 animals/group; combined from 2 independent experiments). $^{*}p$ <0.05, $^{**}p$ <0.01 Mann–Whitney *U* test. Bcl6, B-cell lymphoma 6; O.D., optical density; PNA, peanut agglutin; SR, Sirius red; WT, wild type.

medium/IMDM for 7 days. Cells were then washed and cultured in fresh IMDM containing 2 μM KD025 or DMSO and analysed at the indicated times via the IncuCyte ZOOM System (Essen Bioscience) and the 2016A Live Cell Imaging sofware after application of a scratch.

Statistical analysis

Statistical analyses were performed using Prism version 7 software (GraphPad, San Diego, USA). Differences between 2 groups were evaluated using the Mann–Whitney *U* test, whereas for more than 2 groups, Kruskal–Wallis tests were performed. Data are presented as mean ± SEM. A 2-tailed *p* value of <0.05 was considered statistically significant. Where indicated, 'n' represents number of biological replicates.

A list of antibodies used, and details of standard procedures including immunohistochemistry, RNA isolation, quantitative real-time (qRT)-PCR, ELISA, and Western blots can be found in the supplementary information.

Results

ROCK2 signalling blockade prevents TAA-induced liver fibrosis

In initial experiments, we examined the contribution of ROCK2 signalling to the initiation of TAA-induced liver fibrosis (Fig. 1). Mice were co-administered TAA with vehicle (0.4% methylcellulose, daily oral gavage) or KD025 (100 mg/kg/day, daily oral gavage) for a period of 1 week (Fig. 1A). KD025 treatment significantly reduced TAA-induced collagen deposition in the liver as demonstrated by SR staining and Aperio image analysis (Fig. 1B). Additionally, immunolabelling for alpha smooth muscle actin (α-SMA) and F4/80 demonstrated a significant reduction in

the number of activated myofibroblasts and pericentral F4/80$^+$ monocyte sequestration, respectively, which represent characteristic features of early injury in this model[26] (Fig. 1C and D). Flow cytometric analysis of the immune cell infiltrate into the liver revealed a significant decrease in both myeloid cells and CD3$^+$ T cell populations in livers from KD025-treated mice (Fig. 1E and Fig. S1A). Thus, we demonstrate a critical role for ROCK2 signalling in the initiation of TAA-induced liver fibrosis, highlighting the potential of ROCK2 inhibition as a prophylactic antifibrotic strategy.

KDO25 displays therapeutic potential for the treatment of established liver fibrosis

To establish the therapeutic potential of KD025, mice were treated with TAA for 6 weeks to induce advanced fibrosis and then co-administered TAA with vehicle or KD025 for a further 2 weeks (Fig. 2A). Livers isolated from 6-week TAA-treated mice exhibited extensive collagen deposition and myofibroblast activation as demonstrated by SR and α-SMA immunohistochemical (IHC) staining (Fig. 2B and C). Moreover, pan-keratin staining (CK-wide spectrum screening) identified the development and expansion of a DR at the 6-week time point (Fig. 2D). Notably, between the periods of 6 and 8 weeks, there was no significant progression in collagen deposition, myofibroblast activation, or the DR expansion. However, a brief 2-week administration of KD025 while TAA treatment was continued promoted marked regression of fibrosis as highlighted by SR staining, demonstrating diminished collagen deposition and significant thinning of fibrotic septa (Fig. 2B). Furthermore, SMA$^+$ myofibroblast numbers were significantly reduced, and the DR was attenuated, following KD025 administration (Fig. 2C and D). In parallel with the effects on myofibroblast numbers, KD025 also significantly reduced the expression of collagen type α1 (Col1a2) mRNA in the liver (Fig. 2E), demonstrating inhibition of fibrotic progression. Some temporal discordance with regard to collagen mRNA expression levels and actual collagen deposition comparing between Week 6 and Week 8 in vehicle-treated mice was noted. We speculate that at Week 8 either translation is reduced or collagen turnover is occurring such that the correlation of mRNA and protein levels is imperfect. Nonetheless, KD025 significantly reduced collagen expression at both the mRNA and protein levels. In line with this, the inflammatory infiltrate was again reduced in response to therapeutic KD025 administration (Fig. 2F and Fig. S1B), although at this time point, the effects were restricted to the myeloid compartment with no alteration in the lymphoid populations observed (Fig. S1C).

ROCK2 targeting inhibits STAT3 phosphorylation and RORγT expression

The mechanisms by which ROCK2 inhibition attenuates liver fibrosis were examined by investigating the expression of its downstream targets. IL-17A represents a pathogenic immunological mediator of fibrosis in multiple disease settings including liver fibrosis. ROCK2 drives an IL-17 differentiation programme through its promotion of STAT3 phosphorylation (pSTAT3) and RORγT expression. Thus, livers harvested from mice administered prophylactic (Fig. 1A) or therapeutic (Fig. 2A) KD025 dosing regimens were analysed for their expression of pSTAT3 and RORγT. In both settings, pSTAT3 and RORγT were decreased in response to KD025 (Fig. 3A and B), although in the prophylactic cohorts, only a trend (p = 0.07) was noted for RORγT (Fig. 3A). Accordingly, qRT-PCR demonstrated a significant decrease in liver IL-17A mRNA expression following KD025 administration in the treatment cohort (Fig. 3C). Next, using IL-17^{cre}Rosa26^{eYFP} fate reporter mice, we demonstrated increased frequency and numbers of CD3$^+$IL-17-expressing T cells in livers from mice treated with TAA for 1 or 6 weeks (Fig. 3D). Notably, KD025 administration resulted in a significant reduction in liver CD3$^+$IL-17A-YFP$^+$ numbers (Fig. 3E). As a profibrotic role for IL-17A in the TAA model has not been previously directly examined, we next used mice globally deficient in IL-17A (IL-17A$^{-/-}$) to confirm the contribution of this cytokine to the initiation and perpetuation of fibrosis. As anticipated, livers from IL-17A$^{-/-}$ mice treated with TAA for 1 or 6 weeks exhibited significantly reduced fibrosis compared with livers from TAA-treated WT mice (Fig. 3F). Together, our findings highlight the attenuation of IL-17 production in the context of inhibited pSTAT3 and RORγT, as a mechanism by which KD025 limits TAA-induced liver fibrosis.

ROCK2 activation is required for BCL6 expression, GC formation, and Ig deposition following TAA treatment

BCL6, an additional target of ROCK2, was significantly increased in livers from mice treated with TAA for 8 weeks plus vehicle for the final 2 weeks compared with those taken at the 6-week time point, and downregulated in response to therapeutic KD025 administration (Fig. 4A). Bcl6 is a transcription factor required for the differentiation of CD4 T cells into Tfh cells, which drive B-cell differentiation and antibody production.[27] Although Tfh/B cell interactions typically occur in GCs in the spleen, recruitment of Tfh to the liver following *Schistosoma japonicum* infection has been reported.[28] The fact that antibodies represent profibrogenic mediators in chronic diseases with fibrotic manifestations such as idiopathic pulmonary fibrosis and systemic sclerosis is well established[29,30]; however, their contribution to liver fibrosis is poorly defined and has not previously been examined in the TAA model.

Notably, therapeutic KD025 administration significantly reduced liver CD19$^+$ B cell numbers (Fig. S2A), highlighting their potential profibrogenic role in liver fibrosis. To address this, we utilised B-cell-deficient mice (uMT$^{-/-}$) and demonstrated reduced severity of liver fibrosis in these animals compared with WT mice after 6 weeks of TAA administration. SR staining demonstrated significantly reduced collagen deposition in livers from uMT$^{-/-}$ mice (Fig. 4B), whereas α-SMA and pan-keratin staining revealed reduced myofibroblast activation and DR development, respectively (Fig. S2C and D). Moreover, following 6 weeks of TAA treatment, circulating IgG levels in WT mice were elevated compared with levels in sera from naïve mice (Fig. 4C). As expected, IgG was undetectable in sera from TAA-treated uMT$^{-/-}$ mice. IHC staining revealed significant IgG deposition within the scar regions in the livers from WT mice treated with TAA for 6 weeks (Fig. 4D). To determine if ROCK2 inhibition by KD025 functioned to attenuate this humoral response, we next performed PNA/CD3/B220 immunofluorescence triple staining to identify GC in spleens from 6-week TAA-treated mice coadministered with TAA and vehicle or KD025 for the final 2 weeks. Consistent with diminished BCL6 expression, confocal imaging showed KD025-disrupted splenic GC formation (Fig. 4E), which was associated with reduced circulating IgG levels (Fig. S2D) and liver IgG deposition (Fig. 4F).

The binding of IgG to Fc gamma receptors (FcγR) on myeloid cells promotes their activation and represents an important pathogenic pathway in autoimmune diseases such as systemic lupus erythematosus and rheumatoid arthritis. As myeloid cells are established mediators of fibrosis in multiple organs and

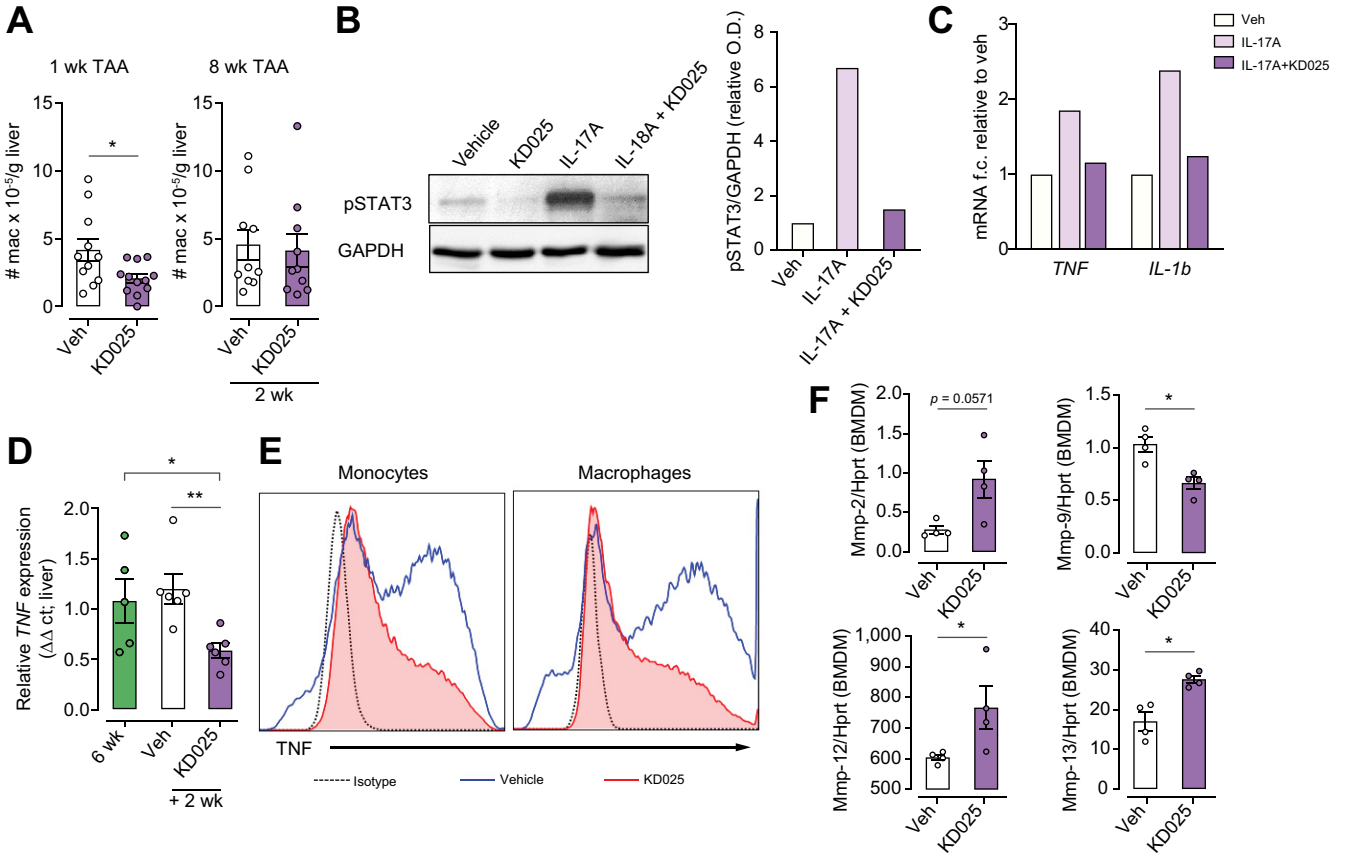

Fig. 5. KD025 alters macrophage function. (A) C57BL/6 mice were treated for 1 week with TAA and vehicle or with TAA and KD025 (left) or were treated with TAA for 6 weeks followed by 2 weeks of TAA co-administration with vehicle or KD025 (right). The number of liver macrophages were quantified (n = 10–12 animals/group; combined from 2 independent experiments). (B) BMDM were treated with DMSO (vehicle), KD025 (10 μM), IL-17A (10 μg/ml), or KD025 + IL-17A for 20 min. Lysates were analysed by immunoblot using antibodies specific for pSTAT3 and GAPDH, with densitometric analyses shown. (C) BMDM were treated with DMSO (vehicle), IL-17A (10 μg/ml), or KD025 (10 μM) + IL-17A for 6 h. qRT-PCR analysis of TNF and IL-1β mRNA normalised to HPRT mRNA is shown. Data shown in (B) and (C) are representative of 2 independent experiments (n = 1/condition). (D) Mice were treated with TAA for 6 weeks or treated with TAA for 6 weeks followed by 2 weeks of co-administration with vehicle or KD025. qRT-PCR analysis of TNF mRNA expression in whole liver (n = 5–6 animals/group) is shown. (E) Isolated hepatic leucocytes from mice treated as in (D) were treated *in vitro* with LPS (100 ng/ml) and analysed by flow cytometry for monocyte (left) and macrophage (right) TNF production. (F) BMDM were treated with KD025 (10 μM) or DMSO control for 6 h, and the expression of mRNAs encoding MMPs, normalised to HPRT mRNA, was determined by qRT-PCR (n = 4 animals/group). Data are presented as mean ± SEM. $^{*}p$ <0.05, $^{**}p$ <0.01 Mann–Whitney *U* test. BMDM, bone marrow-derived macrophages; MMP, matrix metalloproteinase; O.D., optical density; pSTAT3, signal transducer and activator of transcription 3 phosphorylation; qRT-PCR, quantitative real-time PCR; TAA, thioacetamide.

disease settings, and express high levels of Fc receptors, we next queried whether IgG ligation of FcγR contributes to TAA-induced liver fibrosis. Assessment of liver injury in WT and FcγR-deficient ($Fc\gamma R^{-/-}$) mice following 6 weeks of TAA administration demonstrated significantly attenuated fibrosis (Fig. 4G) and myofibroblast activation (Fig. S2E). Notably, in the absence of FcγR, serum IgG levels were significantly elevated (Fig. S2F), suggesting FcγR binding contributes to IgG sequestration in the liver. In line with this, TAA-induced IgG deposition was markedly reduced in livers from $Fc\gamma R^{-/-}$ mice (Fig. S2G). Taken together, our data demonstrate that in addition to inhibiting IL-17 production, ROCK2 inhibition attenuates TAA-induced fibrosis through the disruption of pathogenic antibody production in the context of impaired GC B-cell development.

KD025 alters macrophage function through both direct and indirect mechanisms

We have previously reported a critical role for colony stimulating factor-1 (CSF-1)-dependent monocytes and macrophages in the TAA liver fibrosis model.[26] As reported above, our analysis of the inflammatory infiltrate demonstrated reduced numbers of liver monocytes in response to either preventative or therapeutic KD025 administration regimes. Analysis of liver macrophages in these settings showed that although KD025 modestly reduced macrophage numbers at the 1-week time point, macrophage numbers following therapeutic KD025 administration from 6 to 8 weeks during TAA were unchanged (Fig. 5A). In response to TAA administration, BMDM infiltrate the liver and, over time, increasingly contribute to the macrophage pool.[26] Using Tim4 expression to distinguish Kupffer cells ($Tim4^{+}$) from BMDM ($Tim4^{neg}$), we additionally observed no impact of therapeutic KD025 administration on macrophage subset composition (Fig. S3). Therefore, in further experiments, we addressed whether the protective effects of KD025 are, in part, mediated through the attenuation of profibrogenic macrophage function rather than decreasing macrophage numbers, or altering macrophage composition. In addition to its role in driving IL-17 differentiation, the STAT3 signalling pathway contributes to

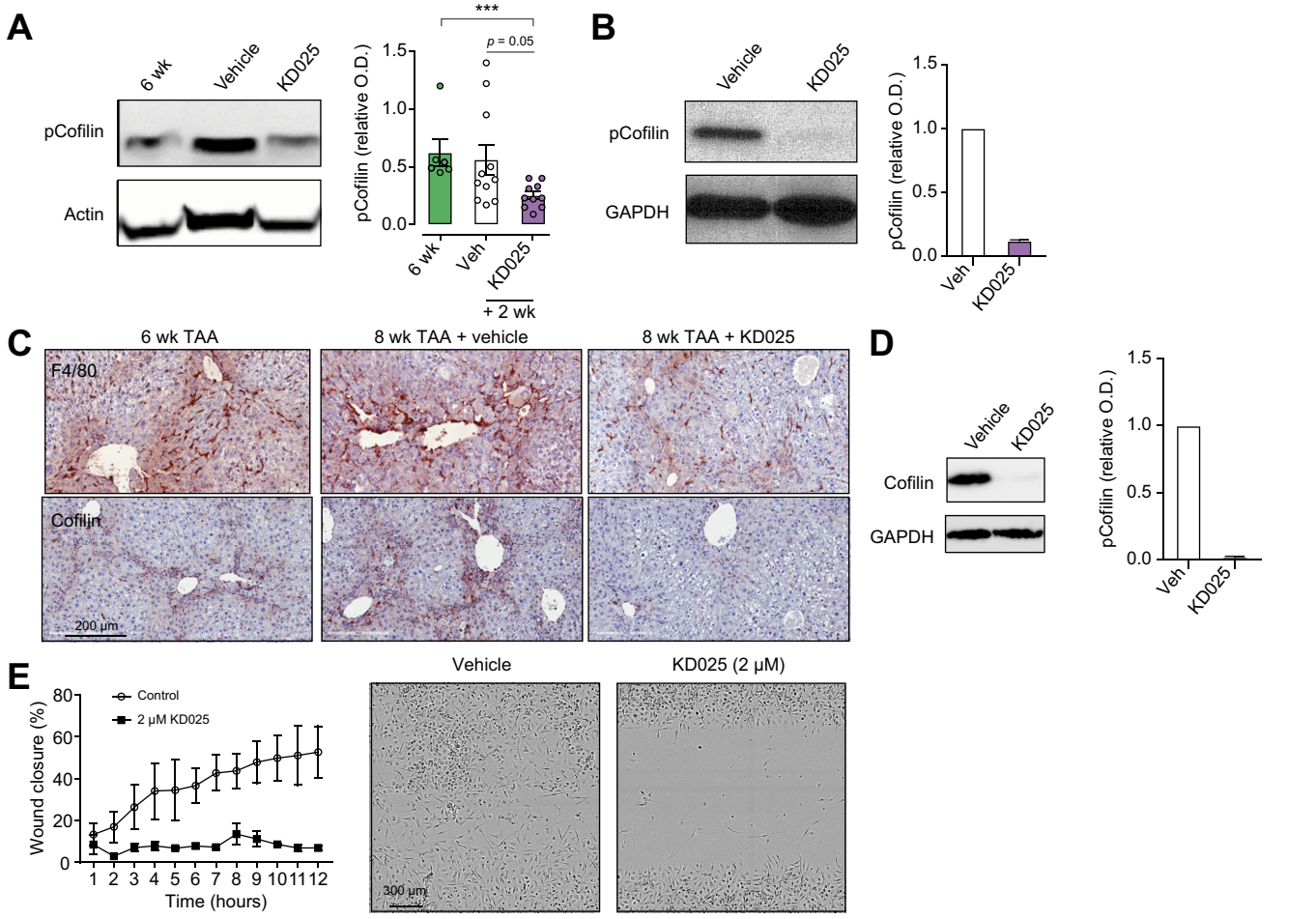

Fig. 6. KD025 alters macrophage migration. (A) C57BL/6 mice were treated with TAA for 6 weeks or treated with TAA for 6 weeks followed by 2 weeks of co-administration with vehicle or KD025. Livers lysates were analysed for the level of pCofilin and actin. A representative immunoblot and densitometric analysis of pCofilin normalized to actin is shown (n = 6–11 animals/group). Data are presented as mean ± SEM. ***p <0.001 Mann–Whitney U test. (B) BMDM were treated with 10 μM KD025 or with DMSO (veh) for 20 min. Levels of pCofilin and GAPDH were determined by immunoblot. A representative blot and densitometric analysis are shown (n = 2 animals/group). (C) Mice were treated as in (A), and liver sections were analysed by histochemical staining for total cofilin. (D) BMDM were treated with KD025 (2 μM) of DMSO (veh) for 6 h, and total cofilin and GAPDH levels were assessed by immunoblot. A representative blot and densitometric analysis of cofilin normalized to GAPDH is shown (n = 2 animals/group). (E) Migration of BMDM in the presence of DMSO (veh) or 2 μM KD025 was assessed over 12 h by scratch wound assay and Incucyte microscopic analysis (n = 3 animals/group). Representative images at 8 h are shown. BMDM, bone marrow-derived macrophages; pCofilin, phosphorylated cofilin; O.D., optical density; TAA, thioacetamide.

altered functionality of cells of multiple lineages including macrophages.[31,32] Importantly, IL-17 signalling in macrophages drives pSTAT3 and promotes pro-inflammatory cytokine production both *in vitro* and *in vivo*.[33,34] Here, we demonstrate ROCK2 inhibition by KD025 ablates IL-17 induced pSTAT3 and TNF and IL-1β mRNA production in CSF-1-elicited BMDM (Fig. 5B and C). Moreover, the expression of TNF, a potent profibrotic cytokine that contributes to liver fibrosis through the perpetuation of inflammation and direct activation of HSCs, was significantly decreased in livers following KD025 administration from Weeks 6 to 8 of TAA treatment (Fig. 5D). Subsequent FACS analysis of liver mononuclear cells isolated from digested livers from these mice revealed that KD025 affected a substantial reduction in lipopolysaccharide (LPS)-elicited macrophage TNF secretion (Fig. 5E). Taken together, these data suggest macrophage intrinsic and extrinsic roles for ROCK2 in altering macrophage function during fibrosis.

Macrophages represent an important source of matrix metalloproteinases (MMPs), which are involved in ECM turnover required for the reversal or repair of fibrotic injury.[15] Examination of MMP mRNA expression profiles in BMDM in response to KD025 treatment demonstrated a significant increase in MMP12 and MMP13 expression, and a trend toward increased MMP2, whereas MMP9 expression was decreased, in response to ROCK2 inhibition (Fig. 5F). This suggests that ROCK2 drives a macrophage phenotype that leads to inefficient matrix turnover as a result of attenuated MMP expression. Moreover, the capacity of KD025 to promote fibrotic regression may be explained in part by restoring macrophage MMP production.

KD025 alters macrophage migration by inhibiting the phosphorylation of cofilin

Cofilin, a target of ROCK2, is implicated in cytoskeletal remodelling during fibrosis.[35] Western blot analysis of whole livers

from mice receiving therapeutic dosing of vehicle or KD025 demonstrated a significant reduction in phosphorylated cofilin (pCofilin) following ROCK2 inhibition (Fig. 6A). Further, we demonstrate constitutive pCofilin expression in BMDM, which was profoundly decreased in response to KD025 exposure (Fig. 6B). As cofilin is an established mediator of macrophage adherence and motility,[36] and macrophages accumulate in the collagen scars of fibrotic livers, we next examined the distribution of liver macrophages in livers from cohorts of mice receiving the therapeutic KD025 administration. IHC staining for F4/80 confirmed F4/80$^+$ macrophage sequestration within the fibrotic septa in fibrotic livers (6 weeks and 8 weeks + vehicle). In contrast, following KD025 treatment, scar-associated macrophages were significantly reduced, with macrophages being more evenly distributed throughout the tissue (Fig. 6C). Furthermore, IHC analysis of total cofilin expression in fibrotic livers demonstrated localised expression within the fibrotic scar regions where macrophages reside and the ablation of cofilin expression by ROCK2 inhibition.

As cofilin expression appeared to colocalise with macrophages, we investigated whether KD025 could modulate cofilin expression and activity in BMDM. Again, using Western blotting, we demonstrated constitutive cofilin expression in BMDM and its inhibition by KD025 (Fig. 6D). In previous studies, it has been demonstrated that cell adhesion to ECM, together with cell spreading, induces ROCK activity.[37] Hence, the strong adherence of BMDM to the tissue culture plastic may be driving ROCK2 activity, thus explaining the constitutively high levels of pCofilin and cofilin in these cells. We therefore examined pCofilin and cofilin levels in peritoneal macrophages (pMac), either freshly isolated from the peritoneal cavity of naïve mice or following short-term culture to allow adherence. We observed minimal levels of both cofilin and pCofilin in freshly isolated *ex vivo* pMac, confirming that short-term adherence was sufficient to induce cofilin expression and its phosphorylation (Fig. S4A), and this process was inhibited by KD025 treatment (Fig. S4B).

As ROCKs are implicated in regulating the motility of multiple cell types, including macrophages, and macrophage distribution in the injured liver was altered following KD025 administration, we examined the contribution of ROCK2 to macrophage migratory capacity. Thus, we performed a scratch wound assay and assessed the impact of KD025 on BMDM migration. Time lapse imaging by phase contrast microscopy showed the migration of BMDM was significantly impeded by KD025-mediated ROCK2 inhibition (Fig. 6E). Together, our data suggest that during fibrosis, in addition to altering macrophage phenotype, ROCK2 effects on the cofilin pathway promote macrophage adherence and migration, thus contributing to their sequestration within fibrotic septae.

Discussion

Hepatocyte injury or death triggers the development of chronic inflammation characterised by imbalanced pro-inflammatory immune response and inability to return to immune homoeostasis. It is now well established that several immune cell types such as macrophages, T helper 17 (Th17)/Tfh cells and B cells drive liver fibrosis via secretion of pro-inflammatory cytokines and other mediators leading to trans-differentiation of HSCs into activated fibroblasts or myofibroblasts and aberrant accumulation of ECM. Therefore, dual targeting of inflammation and fibrogenesis might represent a strategic means to efficiently attenuate and even reverse liver fibrosis in patients. In this study, we demonstrate the pleiotropic role of ROCK2 in the development and perpetuation of liver fibrosis in mice and report the remarkable capacity for therapeutic ROCK2 inhibition to reverse the disease through its integral effects on multiple pro-inflammatory immune cell subsets.

ROCK signalling alters cell function in multiple lineages where functional outcomes are cell type specific. As attenuated fibrosis in response to ROCK1/2 inhibition was shown to be associated with HSC inactivation[38] and cell-intrinsic ROCK signalling in HSCs drives α-SMA and collagen expression,[39] more recent studies have focused on HSC-targeted delivery of ROCK inhibitors as a therapeutic strategy.[40,41] In these studies, the ROCK pathway was confirmed a targetable driver of liver fibrosis in multiple settings and the contribution of cell-intrinsic ROCK signalling in HSCs was demonstrated. However, the contribution of ROCK signalling in upstream immune mediators, and the specific role of ROCK2, the isoform shown to drive pathogenic T-cell,[12,42] B-cell,[43] and macrophage[20] differentiation, in liver fibrosis has not previously been established.

In line with a multitude of clinical and preclinical studies across multiple models of liver fibrosis,[44] fibrogenesis in the TAA model is critically dependent on CSF-1-dependent monocytes/macrophages. We observed that therapeutic administration of KD025 from 6 to 8 weeks during TAA did not alter Kupffer cell or BMDM numbers in the liver but significantly reduced the expression of TNF, a potent profibrotic cytokine that contributes to liver fibrosis through the perpetuation of inflammation and direct activation of HSCs in liver. Furthermore, selective ROCK2 inhibition reduced TNF-α production induced by IL-17 and LPS in CSF-1-dependent BMDM and liver mononuclear cells, respectively. Consistent with ROCK involvement in regulation of cell motility, KD025 treatment robustly reduced cell migration, which was associated with downregulation of cofilin phosphorylation in BMDM. These data suggest that during fibrosis, ROCK2 not only skews the macrophage phenotype toward pro-inflammatory/profibrogenic but also promotes macrophage migration, thus contributing to their sequestration within fibrotic septae in the injured liver. Although we saw no effect on liver macrophage numbers, our data indicate that ROCK2 inhibition with KD025 altered macrophage function through direct and indirect mechanisms without significant cell depletion. Because macrophages can also play positive roles during liver injury and repair, targeting the molecular programmes underpinning pathogenic monocyte/macrophage differentiation, while leaving these populations intact for beneficial function, represents an attractive therapeutic strategy.

A growing body of evidence suggests that IL-17 plays a central role in orchestrating the intrahepatic immune response and exacerbating inflammatory reactions upon liver injury. The expression of IL-17 receptor has been observed on parenchymal and non-parenchymal cells including hepatocytes, HSCs, Kupffer cells, and endothelial cells, all of which drive both inflammation and fibrosis.[45] It has been previously reported that ROCK2 specifically contributes to the regulation of IL-17 secretion in both mice and humans via STAT3- and IRF4-dependent mechanisms.[46] Here, in our studies, we confirmed a pathophysiologic role for IL-17A in TAA-induced liver fibrosis, as livers from IL-17A $^{-/-}$ mice treated with TAA exhibited significantly reduced fibrosis compared with livers from TAA-treated WT mice. STAT3 and RORγT are transcription factors that work in concert to promote T-cell IL-17 differentiation. ROCK2 inhibition disrupted this axis

in TAA-treated mice as demonstrated by a significant reduction in liver pSTAT3, RORγT, and IL-17 levels following either prophylactic or therapeutic administration of KD025. Moreover, KD025 attenuated IL-17-induced pSTAT3 in purified BMDM *in vitro*, suggesting that ROCK2 is implicated in IL-17 signalling in macrophages and potentially can function as an amplifier or feed-forward mechanism of sustained pro-inflammatory immune response.

Although hepatic infiltration by T and B cells parallels parenchymal injury and fibrosis, the precise role of humoral immune response involving Tfh and B cells in development of liver fibrosis is poorly understood. Both STAT3 and Bcl6 transcription factors are required for development of Tfh cells, which support B cell activation and antibody production in GC. We found that B-cell-deficient mice ($uMT^{-/-}$) demonstrated reduced severity of liver fibrosis compared with WT mice after 6 weeks of TAA administration. The reduction in fibrosis was associated with almost undetectable levels of circulating IgGs, significantly reduced collagen deposition, and myofibroblast activation. In contrast, TAA treatment of WT mice resulted in robust IgG deposition within the scar regions in the livers. It has been reported that ROCK2 signalling is required for Tfh function and GC formation in an autoimmune setting via a STAT3/Bcl6-dependent mechanism. In the TAA model, we observed upregulation of Bcl6 expression in livers after 8 weeks of TAA treatment, which was downregulated by therapeutic KD025 administration. These data are in line with recently published findings demonstrating liver-specific ablation of Bcl6 suppresses the progression of non-alcoholic steatohepatitis (NASH) in mice.[47] ROCK2 inhibition also disrupted GC B-cell development as well as pathogenic antibody production and sequestration in the liver. The interaction of IgG with Fc gamma receptor on macrophages activates their pro-inflammatory phenotype and potentially contributes to fibrogenesis. Indeed, FcγR-deficient mice demonstrated significantly diminished liver fibrosis, myofibroblast activation, and IgG deposition compared with WT mice treated with TAA for 6 weeks. Thus, in addition to direct pro-inflammatory effects in macrophages, ROCK2 signalling promotes IL-17 and IgG production in response to TAA, leading to profibrogenic macrophage activation in the liver via these 2 indirect mechanisms, both of which were inhibited by KD025.

In summary, in the present study, we demonstrate the critical role of ROCK2 in promoting liver fibrosis induced by TAA administration through its direct and indirect effects on profibrogenic macrophages. Selective ROCK2 inhibition downregulated pro-inflammatory cytokine secretion and migration in macrophages without a robust cell depletion in the liver. ROCK2 signalling was also implicated in IL-17 signalling, B-cell activation and antibody production, which indirectly contributes to sustained inflammation, ECM deposition, and development of liver fibrosis. In addition to defining the role of ROCK2, in this study, we also provided important and previously undocumented insights into our understanding of cellular mechanisms underpinning liver fibrosis. By using knockout mice, we demonstrated that the downregulation of IL-17, B cells, and Fc ligation resulted in robustly diminished TAA-induced liver fibrosis. Importantly, ROCK2 targeting was shown to be effective in prevention and reversal of TAA-induced liver fibrosis, which models key features of human liver fibrosis, including inflammation and progression of fibrosis to cirrhosis, with evidence for regression. Importantly, the clinical development of belumosudil (generic name for KD025) for autoimmune and fibrotic disorders has advanced significantly in the last 5 years, and it has recently received FDA approval for the treatment of patients with cGVHD. These data together with recent advances in clinical development underscore the therapeutic potential of selective ROCK2 inhibition for chronic liver diseases.

Abbreviations

α-SMA, alpha smooth muscle actin; ALT, alanine aminotransferase; AST, aspartate aminotransferase; Bcl6, B-cell lymphoma 6; BMDM, bone marrow-derived macrophages; cGVHD, chronic graft-*vs*-host disease; CLD, chronic liver disease; Col1a2, collagen type α1; DR, ductular reaction; ECM, extracellular matrix; GC, germinal centre; HCC, hepatocellular carcinoma; HSC, hepatic stellate cell; IHC, immunohistochemical; LPS, lipopolysaccharide; MMP, matrix metalloproteinase; NASH, non-alcoholic steatohepatitis; pCofilin, phosphorylated cofilin; pMac, peritoneal macrophages; pSTAT3, phosphorylated signal transducer and activator of transcription; qRT-PCR, quantitative real-time PCR; RAR, retinoic acid receptor; ROCK, Rho-associated coiled-coil forming protein kinases; ROCK2, Rho-associated kinase 2; RORγt, RAR-related orphan receptor gamma; SR, Sirius red; STAT3, signal transducer and activator of transcription 3; TAA, thioacetamide; Tfh, T follicular helper; TGF-β, transforming growth factor-beta; Th17, T helper 17; TNF, tumour necrosis factor.

Financial support

This work was supported by funding from the National Health and Medical Research Council (1089138) and Cancer Council Queensland (KPAM) and NIH R01 HL11879 and P01 CA142106 (BRB). MWLT was supported by a NH&MRC Career Development Fellowship (1159655).

Conflicts of interest

The authors declare no competing financial interests. BRB receives remuneration as an advisor to Magenta Therapeutics and BlueRock Therapeutics; received research funding from BlueRock Therapeutics, Rheos Medicines, Childrens' Cancer Research Fund, and KidsFirst Fund; and is a co-founder of Tmunity. MN, WC, and AZZ are full-time employees of Kadmon Pharmaceuticals, LLC.

Please refer to the accompanying ICMJE disclosure forms for further details.

Authors' contributions

Designed experiments: CN, WAS, AZZ, KPAM. Performed experiments: CN, WAS, MM, MN, WC, JL, KMI. Analysed data: CN, WAS, MM, MN, WC, JL, AZZ, KPAM. Provided intellectual input: KMI, PB, BRB, ADC, GCM
Provided critical reagents: GRH. Performed blinded histological assessment and quantification of liver pathology: ADC, GCM. Wrote the manuscript: AZZ, KPAM.
Helped write the manuscript: CN, WAS. Reviewed the manuscript: MWLT, KMI, GRH, PB, BRB.

Data availability

Data supporting the findings of this study are available from the corresponding author upon reasonable request.

Acknowledgements

The authors thank Madeleine Flynn for graphic design.

Supplementary data

Supplementary data to this article can be found online at https://doi.org/10.1016/j.jhepr.2021.100386.

References

Author names in bold designate shared co-first authorship

[1] Ishizaki T, Maekawa M, Fujisawa K, Okawa K, Iwamatsu A, Fujita A, et al. The small GTP-binding protein Rho binds to and activates a 160 kDa Ser/Thr protein kinase homologous to myotonic dystrophy kinase. EMBO J 1996;15:1885–1893.

[2] Hoon JL, Tan MH, Koh C-G. The regulation of cellular responses to mechanical cues by Rho GTPases. Cells 2016;5:17.

[3] Riches DW, Backos DS, Redente EF. ROCK and Rho: promising therapeutic targets to ameliorate pulmonary fibrosis. Am J Pathol 2015;185:909–912.

[4] Riento K, Ridley AJ. Rocks: multifunctional kinases in cell behaviour. Nat Rev Mol Cell Biol 2003;4:446–456.

[5] Zhou Y, Huang X, Hecker L, Kurundkar D, Kurundkar A, Liu H, et al. Inhibition of mechanosensitive signaling in myofibroblasts ameliorates experimental pulmonary fibrosis. J Clin Invest 2013;123:1096–1108.

[6] Mera C, Godoy I, Ramírez R, Moya J, Ocaranza MP, Jalil JE. Mechanisms of favorable effects of Rho kinase inhibition on myocardial remodeling and systolic function after experimental myocardial infarction in the rat. Ther Adv Cardiovasc Dis 2016;10:4–20.

[7] Baba I, Egi Y, Utsumi H, Kakimoto T, Suzuki K. Inhibitory effects of fasudil on renal interstitial fibrosis induced by unilateral ureteral obstruction. Mol Med Rep 2015;12:8010–8020.

[8] Zhou H, Fang C, Zhang L, Deng Y, Wang M, Meng F. Fasudil hydrochloride hydrate, a Rho-kinase inhibitor, ameliorates hepatic fibrosis in rats with type 2 diabetes. Chin Med J (Engl) 2014;127:225–231.

[9] Nakagawa O, Fujisawa K, Ishizaki T, Saito Y, Nakao K, Narumiya S. ROCK-I and ROCK-II, two isoforms of Rho-associated coiled-coil forming protein serine/threonine kinase in mice. FEBS Lett 1996;392:189–193.

[10] Knipe RS, Probst CK, Lagares D, Franklin A, Spinney JJ, Brazee PL, et al. The Rho kinase isoforms ROCK1 and ROCK2 each contribute to the development of experimental pulmonary fibrosis. Am J Respir Cell Mol Biol 2018;58:471–481.

[11] **You R**, **Zhou W**, Li Y, Zhang Y, Huang S, Jia Z, et al. Inhibition of ROCK2 alleviates renal fibrosis and the metabolic disorders in the proximal tubular epithelial cells. Clin Sci (Lond) 2020;134:1357–1376.

[12] Chen W, Nyuydzefe MS, Weiss JM, Zhang J, Waksal SD, Zanin-Zhorov A. ROCK2, but not ROCK1 interacts with phosphorylated STAT3 and co-occupies TH17/TFH gene promoters in TH17-activated human T cells. Sci Rep 2018;8:16636.

[13] Tan Z, Qian X, Jiang R, Liu Q, Wang Y, Chen C, et al. IL-17A plays a critical role in the pathogenesis of liver fibrosis through hepatic stellate cell activation. J Immunol 2013;191:1835–1844.

[14] Flynn R, Paz K, Du J, Reichenbach DK, Taylor PA, Panoskaltsis-Mortari A, et al. Targeted Rho-associated kinase 2 inhibition suppresses murine and human chronic GVHD through a Stat3-dependent mechanism. Blood 2016;127:2144–2154.

[15] Wynn TA, Barron L. Macrophages: master regulators of inflammation and fibrosis. Sem Liver Dis 2010;30:245–257.

[16] Nakai K, He Y-Y, Nishiyama F, Naruse F, Haba R, Kushida Y, et al. IL-17A induces heterogeneous macrophages, and it does not alter the effects of lipopolysaccharides on macrophage activation in the skin of mice. Sci Rep 2017;7:12473.

[17] Erbel C, Akhavanpoor M, Okuyucu D, Wangler S, Dietz A, Zhao L, et al. IL-17A influences essential functions of the monocyte/macrophage lineage and is involved in advanced murine and human atherosclerosis. J Immunol 2014;193:4344–4355.

[18] Du J, Paz K, Flynn R, Vulic A, Robinson TM, Lineburg KE, et al. Pirfenidone ameliorates murine chronic GVHD through inhibition of macrophage infiltration and TGF-beta production. Blood 2017;129:2570–2580.

[19] Yang L, Dai F, Tang L, Le Y, Yao W. Macrophage differentiation induced by PMA is mediated by activation of RhoA/ROCK signaling. J Toxicol Sci 2017;42:763–771.

[20] Zandi S, Nakao S, Chun K-H, Fiorina P, Sun D, Arita R, et al. ROCK-isoform-specific polarization of macrophages associated with age-related macular degeneration. Cell Rep 2015;10:1173–1186.

[21] Salguero Palacios R, Roderfeld M, Hemmann S, Rath T, Atanasova S, Tschuschner A, et al. Activation of hepatic stellate cells is associated with cytokine expression in thioacetamide-induced hepatic fibrosis in mice. Lab Invest 2008;88:1192–1203.

[22] Buko VU, Lukivskaya OY, Naruta EE, Belonovskaya EB, Tauschel H-D. Protective effects of norursodeoxycholic acid versus ursodeoxycholic acid on thioacetamide-induced rat liver fibrosis. J Clin Exp Hepatol 2014;4:293–301.

[23] Kitamura D, Roes J, Kühn R, Rajewsky K. A B cell-deficient mouse by targeted disruption of the membrane exon of the immunoglobulin mu chain gene. Nature 1991;350:423–426.

[24] Nakae S, Komiyama Y, Nambu A, Sudo K, Iwase M, Homma I, et al. Antigen-specific T cell sensitization is impaired in IL-17-deficient mice, causing suppression of allergic cellular and humoral responses. Immunity 2002;17:375–387.

[25] Hirota K, Duarte JH, Veldhoen M, Hornsby E, Li Y, Cua DJ, et al. Fate mapping of interleukin 17-producing T cells in inflammatory responses. Nat Immunol 2011;12:255–263.

[26] Melino M, Gadd VL, Alexander KA, Beattie L, Lineburg KE, Martinez M, et al. Spatiotemporal characterization of the cellular and molecular contributors to liver fibrosis in a murine hepatotoxic-injury model. Am J Pathol 2016;186:524–538.

[27] Yu D, Rao S, Tsai LM, Lee SK, He Y, Sutcliffe EL, et al. The transcriptional repressor Bcl-6 directs T follicular helper cell lineage commitment. Immunity 2009;31:457–468.

[28] Chen X, Yang X, Li Y, Zhu J, Zhou S, Xu Z, et al. Follicular helper T cells promote liver pathology in mice during *Schistosoma japonicum* infection. Plos Pathog 2014;10:e1004097.

[29] Kill A, Tabeling C, Undeutsch R, Kühl AA, Gunther J, Radic M, et al. Autoantibodies to angiotensin and endothelin receptors in systemic sclerosis induce cellular and systemic events associated with disease pathogenesis. Arthritis Res Ther 2014;16:R29.

[30] Li FJ, Surolia R, Li H, Wang Z, Kulkarni T, Liu G, et al. Autoimmunity to vimentin is associated with outcomes of patients with idiopathic pulmonary fibrosis. J Immunol 2017;199:1596–1605.

[31] Papaioannou I, Xu S, Denton CP, Abraham DJ, Ponticos M. STAT3 controls COL1A2 enhancer activation cooperatively with JunB, regulates type I collagen synthesis posttranscriptionally, and is essential for lung myofibroblast differentiation. Mol Biol Cell 2018;29:84–95.

[32] Matsukawa A, Kudo S, Maeda T, Numata K, Watanabe H, Takeda K, et al. Stat3 in resident macrophages as a repressor protein of inflammatory response. J Immunol 2005;175:3354–3359.

[33] Chen J, Liao M, Gao X, Zhong Q, Tang T, Yu X, et al. IL-17A induces pro-inflammatory cytokines production in macrophages via MAPKinases, NF-κB and AP-1. Cell Physiol Biochem 2013;32:1265–1274.

[34] Zhang J-Y, Zhang Z, Lin F, Zou Z-S, Xu R-N, Jin L, et al. Interleukin-17-producing CD4(+) T cells increase with severity of liver damage in patients with chronic hepatitis B. Hepatology 2010;51:81–91.

[35] Knipe RS, Tager AM, Liao JK. The Rho kinases: critical mediators of multiple profibrotic processes and rational targets for new therapies for pulmonary fibrosis. Pharmacol Rev 2015;67:103–117.

[36] Jönsson F, Gurniak CB, Fleischer B, Kirfel G, Witke W. Immunological responses and actin dynamics in macrophages are controlled by N-cofilin but are independent from ADF. PloS One 2012;7:e36034.

[37] Bhadriraju K, Yang M, Alom Ruiz S, Pirone D, Tan J, Chen CS. Activation of ROCK by RhoA is regulated by cell adhesion, shape, and cytoskeletal tension. Exp Cell Res 2007;313(16):3616–3623.

[38] Murata T, Arii S, Nakamura T, Mori A, Kaido T, Furuyama H, et al. Inhibitory effect of Y-27632, a ROCK inhibitor, on progression of rat liver fibrosis in association with inactivation of hepatic stellate cells. J Hepatol 2001;35:474–481.

[39] Fukushima M, Nakamuta M, Kohjima M, Kotoh K, Enjoji M, Kobayashi N, et al. Fasudil hydrochloride hydrate, a Rho-kinase (ROCK) inhibitor, suppresses collagen production and enhances collagenase activity in hepatic stellate cells. Liver Int 2005;25:829–838.

[40] Klein S, Van Beuge MM, Granzow M, Beljaars L, Schierwagen R, Kilic S, et al. HSC-specific inhibition of Rho-kinase reduces portal pressure in cirrhotic rats without major systemic effects. J Hepatol 2012;57:1220–1227.

[41] Okimoto S, Kuroda S, Tashiro H, Kobayashi T, Taogoshi T, Matsuo H, et al. Vitamin A-coupled liposomal Rho-kinase inhibitor ameliorates

liver fibrosis without systemic adverse effects. Hepatol Res 2019;49:663–675.
[42] Biswas PS, Gupta S, Chang E, Song L, Stirzaker RA, Liao JK, et al. Phosphorylation of IRF4 by ROCK2 regulates IL-17 and IL-21 production and the development of autoimmunity in mice. J Clin Invest 2010;120:3280–3295.
[43] Weiss JM, Chen W, Nyuydzefe MS, Trzeciak A, Flynn R, Tonra JR, et al. ROCK2 signaling is required to induce a subset of T follicular helper cells through opposing effects on STATs in autoimmune settings. Sci Signal 2016;9:ra73.
[44] Guillot A, Tacke F. Liver macrophages: old dogmas and new insights. Hepatol Commun 2019;3:730–743.
[45] Meng F, Wang K, Aoyama T, Grivennikov SI, Paik Y, Scholten D, et al. Interleukin-17 signaling in inflammatory, Kupffer cells, and hepatic stellate cells exacerbates liver fibrosis in mice. Gastroenterology 2012;143:765–776.e763.
[46] Zanin-Zhorov A, Weiss JM, Nyuydzefe MS, Chen W, Scher JU, Mo R, et al. Selective oral ROCK2 inhibitor down-regulates IL-21 and IL-17 secretion in human T cells via STAT3-dependent mechanism. Proc Natl Acad Sci U S A 2014;111:16814–16819.
[47] Chikada H, Ida K, Nishikawa Y, Inagaki Y, Kamiya A. Liver-specific knockout of B cell lymphoma 6 suppresses progression of non-alcoholic steatohepatitis in mice. Sci Rep 2020;10:9704.